Forensic Science International, 200, 165-176. doi:10.1016/j.forsciint.2010.04.012

Computer assisted photo-anthropometric analyses of full-face and profile facial images

Josh P Davis, Tim Valentine and Robert E Davis

Running head: FACIAL COMPARISON

Author note

Josh P Davis, Department of Psychology and Counselling, University of Greenwich, London, SE9 2UG

Tim Valentine and Robert E Davis, Department of Psychology, Goldsmiths, University of London, London, SE14 6NW United Kingdom

Correspondence concerning this article should be addressed to:

Dr. Josh P Davis, Department of Psychology & Counselling, University of Greenwich, Southwood Site, Avery Hill, Eltham, London, SE9 2UG

Tel: +44 20 8331 8859

Fax: +44 20 8331 8625

E-mail: j.p.davis@gre.ac.uk

Abstract

Expert witnesses using facial comparison techniques are regularly required to disambiguate cases of disputed identification in CCTV images and other photographic evidence in court. This paper describes a novel software-assisted photo-anthropometric facial landmark identification system, *DigitalFace* tested against a database of 70 full-face and profile images of young males meeting a similar description. The system produces 37 linear and 25 angular measurements across the two viewpoints. A series of 64 analyses were conducted to examine whether separate novel *probe* facial images of *target* individuals whose face dimensions were already stored within the database would be correctly identified as the same person. Identification verification was found to be unreliable unless multiple distance and angular measurements from both profile and full-face images were included in an analysis.

Keywords: IDENTIFICATION; CCTV; FACE MAPPING; FACIAL COMPARISON; ANTHROPOMETRY

Introduction

In recent years the interrelated topics of identity and surveillance have regularly been features of the political and news agenda. Widespread instances of identity fraud have led to the implementation of preventative measures such as biometric passports and identity cards. Additional crime reduction initiatives have also resulted in the increasing presence of Closed Circuit Television (CCTV) systems. Both types of image are often used within the criminal justice system for identification purposes, with cases resting on whether a suspect is the individual depicted. Offenders often confess if presented with this type of evidence. However, when cases depend on *disputed* identification in photographs, there are various approaches to resolving the issue, and in the UK specific guidelines have been issued by the Attorney General [1].

Witnesses who know a defendant personally can testify as to identity from photographic evidence and research has regularly found that recognition of highly familiar faces in CCTV images is reliable, even if quality is poor (e.g., [2,3]). Juries can also be encouraged to conclude that images depict the defendant and in the UK, if images are 'sufficiently clear', no other form of identity evidence is required. Jurors and most police officers will be unfamiliar with a suspect and even with high-quality images and with no memory demands, the simultaneous identification matching of unfamiliar people is susceptible to error, resulting in high levels of confident false positive and negative decisions [2,4,5]. Furthermore, the presence of the target in person does not increase the safety of this type of matching judgment [6,7].

Experts in face structure may also provide opinion evidence of identity from examination of evidential images. Commonly known as *facial comparison* or *facial mapping*, this type of evidence is admissible worldwide (e.g., [8]; India: [9]; Italy: [10];

South Africa: [11]; USA: [12,13]) and in the UK more than 500 court reports of this type are prepared per annum [14]. Practitioners often use a combination of three approaches to facial comparison:

With *Morphological comparison,* facial features are graded by shape and size into discrete categories (e.g., [10,12,15]). It is probably the most effective technique with images of poor quality or from different viewpoints, as prominent individuating features remain visible. However, features may possess elements of more than one category, are on the boundary between two, or are unclassifiable. Furthermore, statistical analyses can only be conducted at a nominal level, meaning that discrimination of faces possessing similar characteristics will be problematic. Furthermore, features that successfully discriminate one population from a specific geographical region may not individuate those from another [16].

With *photo-anthropometry* (e.g., [17-21]), proportional analyses of the distances and angles between anatomical landmarks in images are calculated and compared. Precise values can be acquired, allowing confidence assessment and parametric analyses. However, problems are encountered if images are not aligned or facial expressions differ, and therefore a combination of photo-anthropometry and morphological comparison techniques may be of most use for examining two facial images [22].

Finally, with *superimposition* (e.g., [23-25]), one image is projected over another in order to highlight facial similarities, or more saliently, discrepancies as well as the possession, or the lack of facial symmetry. However, disambiguation can be hindered by viewpoint differences or style of presentation such as a slow fade. Superimposition using three-dimensional (3-D) images may be most successful when used in conjunction with anthropometry and morphological comparison. Yoshino and colleagues [24,25] demonstrated viewpoint-matched superimposition of 3-D facial images over traditional camera images, allowing accurate identity judgments. Anthropometrical locations were marked on both images and software automatically extracted a two-dimensional image from the 3-D image for alignment with the camera photograph. Using reciprocal point-to-point distances, the system was found to be 100% accurate at matching a database of 100 disguised photographed faces with 3-D images of the same individuals. Other researchers (e.g., [26]) have found comparable rates of success using 3-D laser scans.

Regardless of method, only proof of non-identity is possible. A single reliable difference has more weight than a multitude of similarities. Even if results suggest that two different images are of the same person, proof of identity cannot be established as fact. Furthermore, CCTV images are often of poor quality, with feature boundaries indistinct, obscured, in shadow or distorted. Posed identity photographs may not suffer from these problems, although source equipment discrepancies, brightness range, colour capture and reproduction can alter appearance. Camera and lens quality, distance, the nature and direction of lighting, blur, pixel resolution with digital images, and analogue tape quality must also be considered. Nevertheless, the greater the number of similarities between two images, the greater the likelihood of an identity match.

Given these issues, it is perhaps not surprising that facial comparison has been criticized, particularly as two or more witnesses using similar techniques can come to opposite conclusions [14,27]. In the UK, judges [28] have called for the establishment of large scale facial measurement databases to calculate the likelihood that two different individuals possess similar face structures. Without this safeguard the court ruled that opinions could be regarded as subjective. However, practitioners often apply their techniques using hand-held equipment such as calipers and constructing such a database might be impractical.

Extensive literature has been published describing automatic face identification algorithms (e.g., [29-31]), some being more accurate than humans under optimal conditions at correctly identity matching or discriminating two different faces when tested against large databases. However, when viewpoint is incongruent, or images are filmed under different environmental conditions, accuracy of computer facial recognition systems is worse than human performance [32,33]. Future innovations may prove successful in eliminating or identifying potential suspects. However, human observers will probably continue to personally examine evidence before testifying in court.

Some photo-anthropometrical measures have been published (e.g., [17-21]), as have reports detailing its successful application in real criminal trials (e.g., [8,12]). Nevertheless, this has mostly involved a limited set of measurements against nonexistent, or small facial databases, containing heterogeneous groups of people unlikely to be the subject of mistaken identifications. Kleinberg et al. [20] analyzed distance and angular measurements derived from a set of four landmarks on a database of 120 male police recruits, concluding that the use of this limited measurement set was less reliable for face discrimination than the application of morphological comparison techniques.

Mardia et al. [18] analyzed a database of 358 young adult white male faces, captured in full-face and profile views taken in a controlled environment. Twenty distance and angular measurements between landmarks were collected. High correlations between all measurements highlighted limitations in face discrimination even with these extremely high-quality viewpoint-standardized images. Full-face and profile viewpoint analyses were conducted separately and if combined, as might be possible if multiple images were acquired in a real legal case, a more robust method may have emerged. Nevertheless, several successful prosecutions have been secured in Australia using a combination of techniques, including fewer than ten anthropometrical measurements [8].

For the current paper, a custom software-assisted facial landmark photo-anthropometric identification system, *DigitalFace* was designed, and was evaluated to examine whether its application could be useful to the courts. With images displayed on a computer monitor, operators identify and save up to 38 facial landmark sites in full-face (*anterior*) view; and 14 landmarks in *profile* view, producing a database of 37 linear and 25 angular measurements, more than the number used in previous published research. Repeated attempts by the same or different operators for reliability analyses are possible and *DigitalFace* can be used with any images taken from the same viewpoint, although it was specifically designed for full-face and profile images, such as police ‘mug shots’. Minimum acceptance criteria for identity determination were generated, tested against a database of 70 male faces meeting a similar description.

Reliability of the system to identify two images (*probe* and *target*) as the same person and not to match a probe with a distracter in the database was examined. *Match* or *mismatch* judgements between items in the database were based on a converted distance in Euclidean space. The Euclidean space is an implementation of the concept of a Face-space, in which the parameters derived by *DigitalFace* form the dimensions of the space [34,35]. Perceptual measures of facial similarity were also acquired of all pairs of database faces. Some had been prone to incorrect identification as the same person by human participants in previous matching experiments [6]. These experiments replicated scenarios that might occur when CCTV evidence has been acquired. Thus, circumstances were similar to cases in which expert witnesses might be requested to assist in determining identity.

There were two criteria for a positive identification decision. Firstly, the probe and target measurements (proportional distances and/or angles) of two images of the same person should be closer in Euclidean space than the distance to any distracter. The second, more rigorous criterion was that the distance between two images of the same person should additionally be less than that between all other pairs of images of two different faces. The latter meets court recommendations for testing against a relevant database to provide an estimate of the likelihood of other members of the population possessing similar attributes. The probe images were of eight young males taken three weeks after their target database photographs had been acquired. Hairstyle had slightly changed and there were minor viewpoint variations as might occur naturally even with posed passport photos. Features may be obscured or unclear in CCTV available from a crime scene and the specific choice of measurements in any facial comparison analysis will depend on availability. Therefore, a series of 64 separate analyses were conducted using alternative measurements, including angular only to assess viewpoint consistency.

Method

Materials

The full-face and profile probe and target photographs were of eight volunteers recruited to a previous identity matching study [6]. All were male white European (aged 18 – 22), of slim or medium/muscular build (72 – 95 kg, 1.70 - 1.92 m), clean-shaven, with brown or black hair, neither receding, nor below collar length. None had distinguishing facial marks or wore jewelry. The probe images were taken approximately three weeks after the target images. Photographs of 62 distracters meeting a similar description were also acquired. All volunteers adopted a neutral expression, while the photographs were taken from approximately 3m with a Samsung Fino 1O5OXL camera on full zoom loaded with black-and-white film. Photographs were scanned and transformed to BMAP files.

For the perceptual measure of facial similarity, the target and distracter full-face photographs had been included with 30 others in an unpublished study in which participants (n = 75) organized the 6” x 4” full-face photographs into categories based on perceived similarity. For efficacy, only 65 of the 100 faces were randomly sorted by each participant. The remaining 35 were provided to the next participant, together with 30 of the 35 sorted by the previous participant. There were no limits on category numbers and unique faces could be left aside as a single category. The number of categories produced by participants ranged from 4 to 53, with a median of 21 and a mode of 29. These data were entered into a 100 x 100 matrix showing the frequency with which each face was matched with another. A high frequency within a cell was indicative of high levels of facial similarity between two different faces. The highest cell frequency was 25 and 3,050 of the 4,950 cells (61.6%) were empty. The mean frequency was 0.75 (SD = 1.64), 26 pairs (.005%) were matched ten times or more, 111 pairs (2.24%), five times or more.

Procedure

Using the DigitalFace system, images were displayed on a 16” monitor screen with landmarks located four times with the system’s maximum zoom setting (zoom x 3), and four times on mid-zoom (zoom x 2). With full zoom, the distance between the pupils of the eyes on the screen was approximately 15 cm. With mid-zoom, it was approximately 10 cm, both larger than in real life. Throughout the process, DigitalFace provides a visual reminder of each landmark to be located, using its ‘common’ name in the order listed in Figure 1 for full-face views and Figure 2 for profile views (listed with anatomical nomenclature). Using a computer mouse, cross hairs are moved until the landmark is located and provisionally saved by clicking on the left mouse and confirmed by clicking on the right mouse. Landmark identification sometimes requires the use of a horizontal or vertical projected line. For instance, measurement of the width of the face is performed by initially selecting an internal landmark (i.e. top of upper lip, Figure 1, Location 13). From this, a line parallel to one connecting the inner eyes is projected onto the screen for identification of the edge of the face at this vertical height (*Figure 1, Locations 14 & 15*). The procedure takes less than 5 minutes.

Following landmark identification, *DigitalFace* automatically exports 14 angular and 25 distance full-face measurements and 11 angular and 12 distance profile measurements (in pixels) into a database. The technique required to measure the distance between a target point and the nearest point to it on any orthogonal base line is reported in Annex 1. Figures 3 (full-face) and 4 (profile) display the distance measurements, Figures 5 (full-face) and 6 (profile) the angular measurements. Those marked with the letter T denote transient measures (e.g., eyebrows; hairline) that are easily manipulated and might be inappropriate to rely on if there is a belief that an offender may have changed appearance.

Outliers on each measurement more than 2 SD from the mean for that face, denoting location errors were removed from further analyses. Median values were retained. As is common with this type of procedure when the precise distance from the target to the camera is not known, distance measurements were expressed as ratios. In full-face view, the vertical proportions were ratios of a distance parallel to a line linking the inner eyes and the chin (*Figure 3*; vertical distance: F13). Horizontal ratios were proportions of the distance between the ears (*Figure 3*; horizontal distance: F8). In profile view, vertical ratios were proportions of the distance parallel to that between the chin and the upper ear (*Figure 4*; vertical distance: P3 + P5). Horizontal ratios were expressed as a proportion of the distance between the tip of the nose and the rear of the ear (*Figure 4*; horizontal distance: P9). Some distance measurements provided by *DigitalFace* overlap. For instance (*Figure 3*), the distance from the bottom of the nose to firstly, the bottom of the lower lip (F12), to secondly, the centre of the mouth (F11); and to thirdly, the upper lip (F10). Multiple overlapping measurements provide flexibility if features are obscured.

To avoid overlap, for the analyses reported in this paper, some distances listed in Figures 3 and 4 were converted into new independent measures (*Table 1*). Thus, one new distance was that from the nose base to the top of the upper lip (FV2), a second, the upper lip height (FV3).

A series of separate Euclidean Distance analyses were conducted. Included in each were one probe, the target and the 69 distracters (71 cases). All measures were standardized so that each was equally weighted and the squared Euclidian distance was computed between each pair of cases. The equation for squared Euclidean distance is as follows:

$$\sum_{i=1}^{v}\left(X_i - Y_i\right)^2 ,$$

This is the sum across variables (from i = 1 to v) of the squared difference between the score on variable i for the one case (X_i) and the score on variable i for the other case (Y_i). A squared Euclidean distance of zero is indicative of an exact match. A high distance indicates a weak relationship. There is no set maximum value as this is dependent on the number of variables, cases and measurement similarities.

Results

General interpretation of photo-anthropometrical analyses

A series of 64 independent analyses were conducted. Each of the eight probe faces were separately included with the database faces (which included the target) to generate a proximity matrix, using eight different sets of measurements as might be necessary with evidence acquired in the course of a criminal investigation (*Tables 2 – 9*). Alternative measures might be preferred in different circumstances. Reported in each table is the squared Euclidean distance between each probe to the target of the same person, as well as the distance between each probe to the nearest distracter in Euclidean space. If the probe-target distance was less than the probe-closest distracter distance, that probe is marked with a single star as this passed the primary criterion for a match. Columns without a star indicate a failure to match the two photographs of the same person and in a forensic investigation would result in a false negative identity decision.

The mean squared Euclidean distance and standard deviation, as well as the maximum and minimum distances between any two different faces within the database are also reported[1]. The minimum value is associated with the secondary more robust criterion for identity decisions, being that the squared Euclidean distance between the probe and target should be less than that between any two database faces. If passed, probes are marked with a double star.

In addition, the number of cases in each proximity matrix is listed in which two different distracters possessed a lower squared Euclidean distance between each other than that between each target and probe is listed. This denotes the number of false alarms potentially associated with each probe if identity judgments were decided entirely on that analysis. Finally, data from the perceptual facial similarity study are also included. This value is the number of participants who matched together the probe and the specific distracter closest in Euclidean space to the target. This provides an indication of the likelihood of a mistaken identification or false alarm by human observers, in that the higher the frequency, the closer the perceived physical resemblance.

Analysis 1: Full-face angular measures only

[1] Whereas the mean squared Euclidean distance across all items in the database remains consistent when the number of variables remains consistent, the maximum, minimum and standard deviation of the mean vary slightly as each probe exerts a different influence on the distribution shape. Those reported in Tables 2 to 9 are the median value for each statistic across the eight analyses. The slight variation in minimum values did not influence any second criterion identity decisions.

Analysis 1, conducted using the 14 full-face angular measurements only (see *Figure 5*), provides an indication of the similarity of viewpoint between each target and its probe. On this test (*Table 2*), four probes (Probes 1, 2, 4 and 8) were closer in Euclidean space to at least one distracter than to their respective targets, indicating some viewpoint misalignment.

The lowest squared Euclidean distance between two different faces in the database, at 1.91 was closer than the distance between seven probes and their respective targets. Only Probe 6 (squared Euclidean distance = 1.49) passed both criteria for a match, indicative of a close consistency of viewpoint.

Analysis 2: Full-face permanent distance measures only

The second analysis assessed the 15 permanent horizontal and vertical full-face distance measures only (see *Table 1*). Four probes passed the secondary criterion (Probes 2, 6, 7, 8), as the distance between each probe and respective target was less than that between the minimum for two different database faces (*Table 3*). Two probes (Probe 1 and 5) were closer in Euclidean space to at least one distracter than to the target photograph of the same person, indicating primary criterion matching failures. Probe 5 was also within the top 1% of highest frequencies in the perceptual similarity database, denoting an extremely high degree of appearance similarity. In a simultaneous matching experiment to video [6], 29.3% of participants had wrongly mistaken one of these two actors to be the other in video. As such, neither human observers nor the limited measurements described in Analysis 2 reliably discriminated between them.

Interestingly, Probe 2 passed both matching criteria and yet in Analysis 1 (*Table 2*) the viewpoint of this pairing was revealed to be the most misaligned.

Analysis 3: Full-face permanent and transient distance measures only

In the third analysis, transient measurements such as those derived from eyebrows (see *Table 1*) were added to those used in Analysis 2. All probes passed the primary matching criterion (*Table 4*), demonstrating that the increase in measurements increases reliability and negates some of the viewpoint differences identified in Analysis 1. Nevertheless, five probes failed the secondary criterion for a match and in addition, some of the probes possessing the closest Euclidean distance to distracters had perceptual similarity ratings in the top 1%, meaning that these were most likely to be mistaken for one another by humans (Probes, 3, 4 & 8).

Analysis 4: All full-face permanent, transient and angular measures

Analysis 4 was conducted with the inclusion of all angular and distance full-face measures (see *Table 1* and *Figure 5*). All probes passed the primary match criterion (*Table 5*). However, two failed the secondary criterion (Probes 1 & 3), indicating that even with the inclusion of all the full-face *DigitalFace* measurements identifying one individual from two images taken from this viewpoint could not be reliably established.

Analysis 5: Profile angular measures only

Analysis 5 was conducted on the profile angular measures only (see *Figure 7*) and was designed to establish a measure of closeness of viewpoint of each probe/target pair. Three probes passed the primary criterion (*Table 6*). None passed the secondary criterion.

Analysis 6: Profile permanent distance measures only

Analysis 6 examined the distance measure data associated with the profile view photographs (see *Table 1*). On this analysis only one of the probes passed both criteria for a match (*Table 7*). Three failed both primary and secondary criteria (Probes 2, 7, 8).

Analysis 7: All profile measurements

For the seventh analysis, the transient distance and angular profile measurements were added to those from Analysis 5 (see *Table 1* and *Figure 7*). All probes passed the primary criteria, with three passing the secondary matching criteria (*Table 8*), demonstrating that similar to the equivalent full-face analysis (Analysis 4), reliable discrimination was not possible using a single photographic viewpoint.

Analysis 8: All full-face and profile permanent and transient measures

All profile and full-face permanent, transient and angular measurements were included in Analysis 8. All probes passed both the primary and secondary matching criteria (*Table 9*). This procedure could only be followed in a forensic investigation if images from different viewpoints were acquired.

Discussion

The findings of the photo-anthropometrical analyses using the *DigitalFace* landmark identification system illustrate that caution is required if deciding whether two different photographs depict the same person. Even when all distance and angular measurements were included in full-face view, and separately with all measurements in profile view, there were a number of failures to match on the robust secondary criteria that the Euclidean distance between a target and a probe should be less than that between any two different database faces. Correct categorization only occurred when both full-face and profile viewpoints were analysed together. However, in many real cases only a single limited view of the offender would be obtained.

The images were posed in a manner acceptable for identity documents and although viewpoint in images of the same person did not exactly match, the high photographic quality allowed for the optimal measurement of a large number of distance and angular measures in both full-face and profile views. Few evidential images, particularly those obtained from CCTV would afford such fine detail and the use of the same camera for probe and target images as in this research will tend to exaggerate performance when compared with most real cases. Indeed, with low-resolution or unclear images such as if the subject is sited some distance from the camera, features are obscured, or viewpoint is not matched, landmark identification would be more problematic, limiting the number of measurements and increasing error likelihood. And yet, cases have progressed in court with experts reporting on the use of far fewer measurements applied to images from a single viewpoint.

Thus, these analyses highlighted difficulties involved in photo-anthropometry due to the commonality of facial proportions, among even this small database. There have been calls for the establishment of large-scale databases of facial measurements in order to assess the safety of facial comparison techniques [28]. Criticism could be directed at the limited size of the database of 70 faces. However, the homogenous inclusion criteria ensured that all distracter faces met the same basic physical description. An increase in database size would probably result in more faces possessing similar facial dimensions, increasing the potential for error. Alternative databases would be necessary if the system was to be applied to those of a different ethnicity, age group or gender. It may also be possible to apply alternative novel statistical techniques [36]. Furthermore, Yoshino and colleagues [25] have suggested that a database of 3-D images, and associated facial measurements could be routinely obtained in a similar manner to police mug-shots. In conjunction with both morphological comparison and anthropometric analysis, an accurate assessment of identity might be achieved against this database, if, using superimposition techniques, an extract from a 3-D image could be accurately aligned over evidential images.

Reliable differences between the faces in the posed images obtained for this research meant it was possible to confidently state that they did not depict the same person. However, measurement differences do not necessarily indicate different people, as viewpoint may not be aligned or appearance may have changed, perhaps caused by hairstyle, aging or cosmetic surgery. Expert witnesses would probably only be asked to apply their techniques when images were impoverished in some manner. Indeed, under UK law, an expert should only be called to present evidence if a task is beyond the expected skills or experience of a judge or jury [37]. If images were of such high-quality as those used here, a jury would probably be invited to make their own unaided visual comparison, a potentially unreliable procedure [5-7].

In conclusion, the use of the *DigitalFace* system provided some assessment of the likelihood of occurrence of people with similar facial characteristics. If presented in court, it would be possible to provide an objective opinion as to identity. From a forensic perspective the number of measurements included in these analyses was higher than would often be obtained in real cases, due to the high quality of the photographs. Furthermore, in many cases, only frontal or profile views would be obtained, not both as reported here, highlighting the need for caution, when attempting to 'prove' an identity match beyond reasonable doubt.

Acknowledgements

This work was funded by a Postgraduate Studentship Grant PTA-030-2002-00990 from the Economic and Social Research Council, UK. Part of this research was presented at the British Psychological Society Annual Conference, University of York in March 2007. We thank two anonymous reviewers for their helpful comments on an earlier version of this work.

List of references

[1] Attorney General's Reference, No.2 of 2002. EWCA Crim 2373, UK (2003)

[2] V. Bruce, Z. Henderson, C. Newman, A.M. Burton, Matching identities of familiar and unfamiliar faces caught on CCTV images, J. Exp. Psychology: App. 7 (3) (2001) 207-218.

[3] A.M. Burton, S. Wilson, M. Cowan, V. Bruce, Face recognition in poor-quality video: Evidence from security surveillance, Psychological Sci. 10 (3) (1999) 243-248.

[4] V. Bruce, Z. Henderson, K. Greenwood, P.J.B. Hancock, A.M. Burton, P. Miller, Verification of face identities from images captured on video, J. Exp. Psychology: App. 5 (4) (1999) 339-360.

[5] Z. Henderson, V. Bruce, A.M. Burton, Matching the faces of robbers captured on video, App. Cognitive Psychology 15 (2001) 445–464.

[6] J.P. Davis, T. Valentine, CCTV on trial: Matching Video Images with the Defendant in the Dock, Appl. Cognitive Psychology 23 (2009) 482–505.

[7] R. Kemp, N. Towell, G. Pike, When seeing should not be believing: Photographs, credit cards and fraud, App. Cognitive Psychology 11 (1997) 211–222.

[8] G. Porter, G. Doran, An anatomical and photographic technique for forensic facial identification, Forensic Sci. Int. 114 (2000) 97–105.

[9] P. Sinha, Symmetry sensing through computer vision and a facial recognition system, Forensic Sci. Int. 77 (1996) 27–36.

[10] F. Ventura, A. Zacheo, A. Ventura, A. Pala, Computerized anthropomorphometric analysis of images: Case report, Forensic Sci. Int. 1468 (2004) S211–S213.

[11] M.M. Roelofse, M. Steyn, P.J. Becker, Photo identification: Facial metrical and morphological features in South African males, Forensic Sci. Int. 177 (2008) 168-175.

[12] R.A. Halberstein, The application of anthropometric indices in forensic photography: Three case studies. J. Forensic Sci. 46 (6) (2001) 1438–1441.

[13] R.W. Vorder Bruegge, T. Musheno, Identification of individuals through photographic facial comparisons, Abstracts - The 9th Scientific Meeting of the International Association for Craniofacial Identification, Washington, DC, 2000. For. Sci. Com. 2 (www.fbi.gov)

[14] M.C. Bromby, At face value? New Law J. Expert Witness Supp. (Feb 28) (2003). 302-303.

[15] P. Vanezis, D. Lu, J. Cockburn, A. Gonzalez, G. McCombe, O. Trujillo, M. Vanezis, Morphological classification of facial features in adult Caucasian males based on an assessment of photographs, J. Forensic Sci. 41 (5) (1996) 786–791.

[16] M.Y. Iscan, The introduction of techniques for photographic comparison: potential problems, in M.Y. Iscan, R.P. Helmer (Eds.), Forensic Analysis of the Skull: Craniofacial Analysis, Reconstruction and Identification. Wiley-Liss, New York, 1993, pp. 57–70.

[17] T. Catterick, Facial measurements as an aid to recognition, Forensic Sci. Int. 56 (1992) 23–27.

[18] K.V. Mardia, A. Coombs, J. Kirkbride, A. Linney, J.L. Bowie, On statistical problems with face identification from photographs, J. App. Statistics 23 (6) (1996) 655–675.

[19] A.M. Burton, V. Bruce, N. Dench, What's the difference between men and women: Evidence from facial measurement, Perception 22 (2) (1993) 153–176.

[20] K.F. Kleinberg, P. Vanezis, A.M. Burton, Failure of anthropometry as a facial identification technique using high-quality photographs, J. Forensic Sci. 52 (4) (2007) 779–783.

[21] K.R. Laughery, B.T. Rhodes, G.W. Batten, Computer-guided recognition and retrieval of facial images, in G.M. Davies, J.W. Shepherd, H.D. Ellis (Eds.), Perceiving and Remembering Faces. Academic Press: New York: (1981).

[22] M.M. Roelofse, M. Steyn, P.J. Becker, Photo identification: Facial metrical and morphological features in South African males. Forensic Sci. Int. 177 (2008) 168-175.

[23] P. Vanezis, C. Brierley, Facial image comparison of crime suspects using video superimposition. Science & Justice 36 (1996) 27-33.

[24] M. Yoshino, H. Matsuda, S. Kubota, K. Imaizumi, S. Miyasaka, Computer-assisted facial image identification system using a 3-D physiognomic range finder. Forensic Sci. Int. 109 (3) (2000) 225–237.

[25] M. Yoshino, K. Noguchi, M. Atsuchi, S. Kubota, K. Imaizumi, C.D.L. Thomas, J.G. Clement, Individual identification of disguised faces by morphometrical matching. Forensic Sci. Int. 127 (1-2) (2002) 97 – 103.

[26] N. Lynnerup, M.L. Clausen, A.M. Kristoffersen, H. Steglich-Arnholm, Facial recognition and laser surface scan: a pilot study. For. Sci. Med. Pathol. 5 (2009) 167-173.

[27] A. Campbell-Tiech, Stockwell revisited: The unhappy state of facial mapping, Archbold News 6 (2005) 4–6.

[28] R v Gray, EWCA Crim 1001, UK (2003)

[29] R. Brunelli, T. Poggio, Face recognition: Features versus templates. IEEE Trans. Pattern Analysis Mach. Int. 15 (10) (1993) 1042–1052.

[30] B. Heisele, P. Ho, J. Wu, T. Poggio, Face recognition: Component-based versus global approaches, Comp. Vision Image Understanding, 91 (1 - 2) (2003) 6-21.

[31] L. Wiskott, J.M. Fellous, N. Kruger, C. von der Malsburg, Face recognition by elastic bunch graph matching, IEEE Trans. Image Analysis Mach. Int. 19 (7) (1997) 775–779.

[32] A.M. Burton, P. Miller, V. Bruce, P.J.B. Hancock, Z. Henderson, Human and automatic face recognition: A comparison across image formats, Vision Res. 41 (2001) 3185-3195.

[33] P.J. Phillips, W.T. Scruggs, A.J. O'Toole, P.J. Flynn, K.W. Bowyer, C.L. Schott, M. Sharpe, FRVT 2006 and ICE 2006: Large-scale results, Nat. Inst. Stand. Tech. Tech. Rep. ISTIR 7408 (2007) (http://iris.nist.gov).

[34] T. Valentine, A unified account of the effects of distinctiveness, inversion and race in face recognition, Quart. J. Exp. Psychology 43A (1991) 161-204.

[35] T. Valentine, Face-space models of face recognition, in M.J. Wenger, J.T. Townsend (Eds.), Computational, geometric, and process perspectives on facial cognition: Contexts and challenges Mahwah: LEA. (2001) (pp. 83-113).

[36] R.J. Allen, Exact solutions to Bayesian and maximum likelihood problems in facial identification when population and error distributions are known, Forensic Sci. Int. 179 (2-3) (2008) 211-218.

[37] R v Turner, 60 Cr App R 80 CA, UK (1975)

Table 1: List of converted distances, the codes refer to measures listed in Figure 3 and 4.

Full-face distance measures			
Permanent horizontal distances			
FH1	Inner eyes distance (F1)	FH2	Nose width minus inner eyes (F2) - (F1)
FH3	Mouth width minus nose width (F3) - (F1/2)	FH4	Inter-pupil distance minus mouth (F4) - (F1/3)
FH5	Outer eyes minus inner-pupil (F5) - (F1/4)	FH6	Width at upper lip height minus eyes (F6) - (F1/5)
FH7	Width at nostril height minus upper lip height width (F7) - (F1/6)	FH8	Distance between ears minus width at nostril height (F8) - (F1/7)
Permanent vertical distances			
FV1	Eyeline to nose base (F9)	FV2	Nose base to upper lip (F10 – F9)
FV3	Upper lip height (F11 – F10)	FV4	Lower lip height (F12 – F11)
FV5	Chin to lower lip (F13 – F12)	FV6	Right ear height (F14)
FV7	Left ear height (F15)		
Transient distances			
FTV1	Eyeline to hairline (FT16)	FTV2	Head top to hairline (FT25 – FT16)
FTH1	Face width at eyebrow (FT17)	FTH2	Right eyebrow height (FT18)
FTH3	Left eyebrow height (FT19)	FTH4	Right eyebrow width (FT20)
FTH5	Left eyebrow width (FT21)	FTH6	Between eyebrow distance (FT22)
FTH7	Eyeline to right eyebrow (FT23)	FTH8	Eyeline to left eyebrow (FT24)
Profile distance measures			
Permanent horizontal distances			
PH1	Nose width (P9 – P8)	PH2	Outer eye to rear nose (P8 – P7)
PH3	Front ear to outer eye (P7 – P6)	PH4	Ear width (P6)
Permanent vertical distances			
PV1	Chin to mouth (P5 – P4)	PV2	Mouth to nose base (P4)
PV3	Nose base to nose tip (P1)	PV4	Nose tip to outer eye (P2 – P1)
PV5	Outer eye to upper ear (P3 – P2)	PV6	Nose height (P10)
Transient distances			
PVT1	Top of head to upper ear (PT12 – P3)	PHT1	Eyebrow width (PT11)

Tables 2 - 9: Squared Euclidean distances from the eight probes to their respective targets in the database, to the nearest distracter as well as the number of database cells with pairs of different faces closer in distance than that between probe and target. Also provided are the minimum, maximum and mean (SD) distances between any two different faces on the database. Probes marked with one, or two stars indicate passing respectively the primary; and secondary, criteria for a match. The number of perceptual similarity matches from the probe to the closest distracter is also included.

Table 2: All14 full-face angular measurements

Probe No.	1	2	3*	4	5*	6**	7*	8
Distance to Target	5.69	6.99	3.54	4.00	3.97	1.49	1.96	5.87
Database cells closer in distance	31	63	8	10	9	0	2	37
Distance to closest distracter	4.85	4.25	6.00	3.95	4.25	4.40	5.44	5.81
Similarity matches	7	3	0	3	5	0	1	0
	Max	125.91	*Min*	1.91	*M*	28.00	*SD*	17.71

Table 3: All 15 full-face permanent distance measurements

Probe No.	1	2**	3*	4*	5	6**	7**	8**
Distance to Target	6.88	2.65	10.03	3.25	5.37	0.89	2.27	1.57
Database cells closer in distance	18	0	97	2	7	0	0	0
Distance to closest distracter	6.13	13.00	10.82	6.71	4.48	5.62	8.13	4.39
Similarity matches	4	4	11	3	7	3	7	0
Max	138.66	*Min*	2.77	*M*	30.00	*SD*	15.63	

Table 4: All25 full-face permanent and transient distance measurements

Probe No.	1*	2**	3*	4*	5*	6**	7**	8*
Distance to Target	12.62	3.21	18.75	9.45	12.51	5.65	4.28	7.78
Database cells closer in distance	16	0	44	1	4	0	0	1
Distance to closest distracter	16.10	21.67	20.75	16.57	13.42	16.51	13.28	13.86
Similarity matches	0	4	11	10	2	7	0	13

Max 151.14 *Min* 6.89 *M* 50.00 *SD* 21.26

Table 5: All 39 full-face angular and distance measurements

Probe No.	1*	2**	3*	4**	5**	6**	7**	8**
Distance to Target	18.32	7.46	22.29	13.45	16.48	7.14	6.24	13.65
Database cells closer in distance	1	0	4	0	0	0	0	0
Distance to closest distracter	28.17	33.98	29.49	21.46	26.96	26.08	26.01	27.97
Similarity matches	1	4	0	3	5	7	7	13
	Max	241.71	*Min*	16.86	*M*	78.00	*SD*	32.41

Table 6: All11 profile angular measurements

Probe No.	1	2	3	4	5*	6*	7	8*
Distance to Target	3.93	4.44	11.16	2.33	1.34	3.87	1.45	1.89
Database cells closer in distance	53	49	544	17	4	53	5	7
Distance to closest distracter	1.96	3.86	5.80	1.84	4.22	5.78	0.83	9.87
Similarity matches	4	3	0	1	0	7	10	1
	Max	120.34	*Min*	0.70	*M*	22.00	*SD*	13.99

Table 7: All 10 profile permanent distance measurements

Probe No.	1*	2	3**	4*	5*	6*	7	8
Distance to Target	5.02	5.19	1.89	2.65	2.85	4.87	1.89	5.22
Database cells closer in distance	71	79	0	9	11	70	1	75
Distance to closest distracter	6.34	3.78	2.58	7.11	4.84	24.20	1.80	3.66
Similarity matches	0	3	0	3	0	4	1	2

Max 66.85 *Min* 1.89 *M* 20.00 *SD* 10.67

Table 8: All 23 profile measurements

Probe No.	1*	2*	3*	4**	5**	6*	7**	8*
Distance to Target	9.02	11.22	13.24	5.29	4.96	9.33	3.91	8.37
Database cells closer in distance	7	20	35	0	0	9	0	6
Distance to closest distracter	16.92	18.11	19.71	14.38	10.91	30.92	16.09	21.80
Similarity matches	1	4	1	2	0	7	10	1
	Max 172.53		*Min* 5.35		*M* 46.00		*SD* 20.87	

Table 9: All 62 full-face and profile angular and distance measurements

Probe No.	1**	2**	3**	4**	5**	6**	7**	8**
Distance to Target	27.34	18.69	35.53	18.75	21.44	16.47	10.15	22.02
Database cells closer in distance	0	0	0	0	0	0	0	0
Distance to closest distracter	45.09	65.55	69.03	44.80	44.58	57.00	54.16	67.72
Similarity matches	1	3	0	3	2	7	7	1
	Max	278.96	*Min*	36.43	*M*	124.00	*SD*	39.49

Figure 1: Locations of full-face (anterior) landmarks: Common names given in DigitalFace instructions (with anatomical definitions). Note: right and left locations are from the perspective of the viewer

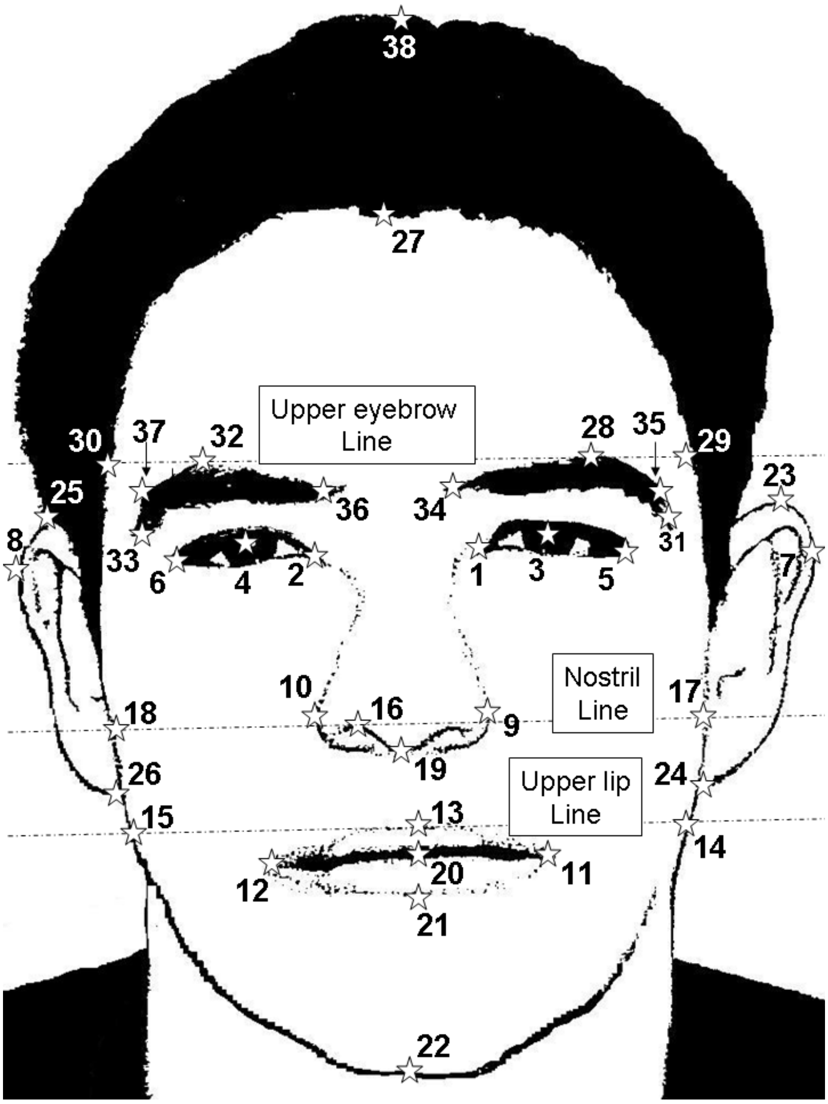

1. Right inner eye (*r endocanthian*) **2.** Left inner eye (*l endocanthian*) **3.** Right pupil centre **4.** Left pupil centre **5.** Right outer eye (*r exocanthian*) **6.** Left outer eye (*l exocanthian*) **7.** Right outer ear (*r postaurale*) **8**. Left outer ear (*l postaurale*) **9.** Right most outer point of nasal area (*r alare*) **10.** Left most outer point of nasal area (*l alare*) **11.** Right outer mouth (*r cheilion*) **12.** Left outer mouth (*l cheilion*) **13.** Top of upper left lip (*l superior labiale*) **14.** Right edge of face at upper lip line **15.** Left face edge at upper lip line **16.** Centre of left nostrum (*l supra subalare*) **17.** Right edge of face at nostril line **18.** Left face edge at nostril line **19.** Nose base (*subnasale*) **20.** Centre of mouth (*stomion*) **21**. Lower lip base (*inferior labiale*) **22.** Chin (*gnathion*) **23**. Right ear top (*r superaurale*) **24.** Right ear base (*r subaurale*) **25.** Left ear top (*l superaurale*) **26**. Left ear base (*l subaurale*) **27.** Hair line at forehead midpoint (*trichion*) **28.** Right eyebrow top (*r superciliare*) **29.** Right face edge on eyebrow top line at hair contact **30.** Left face edge on eyebrow top line at hair contact **31.** Right eyebrow base (*r orbitale superious*) **32.** Left eyebrow top (*l superciliare*) **33.** Left eyebrow base (*l orbitale superious*) **34.** Right inner eyebrow **35.** Right outer eyebrow (*r frontotemporale*) **36.** Left inner eyebrow **37.** Left outer eyebrow (*l frontotemporale*) **38.** Highest point on head (*vertex*).

Figure 2: Locations of profile facial landmarks: Anatomical definitions and common names given in instructions to DigitalFace

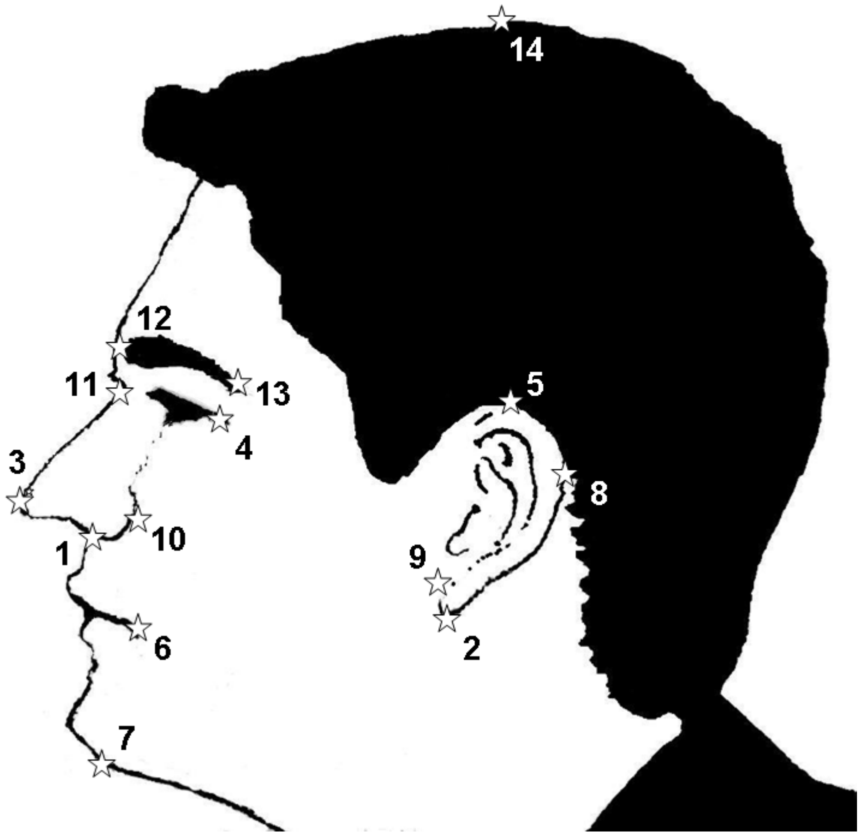

1. Nose base (*subnasale*) **2.** Ear base (*subaurale*) **3.** Nose tip (*pronasale*) **4.** Outer eye (*exocanthian*) **5.** Ear top (*superaurale*) **6.** Mouth corner (*cheilion*) **7.** Chin (*gnathion*) **8.** Ear rear (*postaurale*) **9.** Front of ear, point of attachment of ear lobe to cheek (*otobasion infrious*) **10.** Most lateral point of the curved part of the nose alar (*alar curvature*) **11.** Deepest landmark at the top of the nose (*sellion*) **12.** Prominent midpoint of eyebrows (*glabella*) **13.** Outer eyebrow (*frontotemporale*) **14.** Highest point on head (*vertex*)

Figure 3: Permanent and transient (marked with a T) distance measures produced by DigitalFace in full-face view

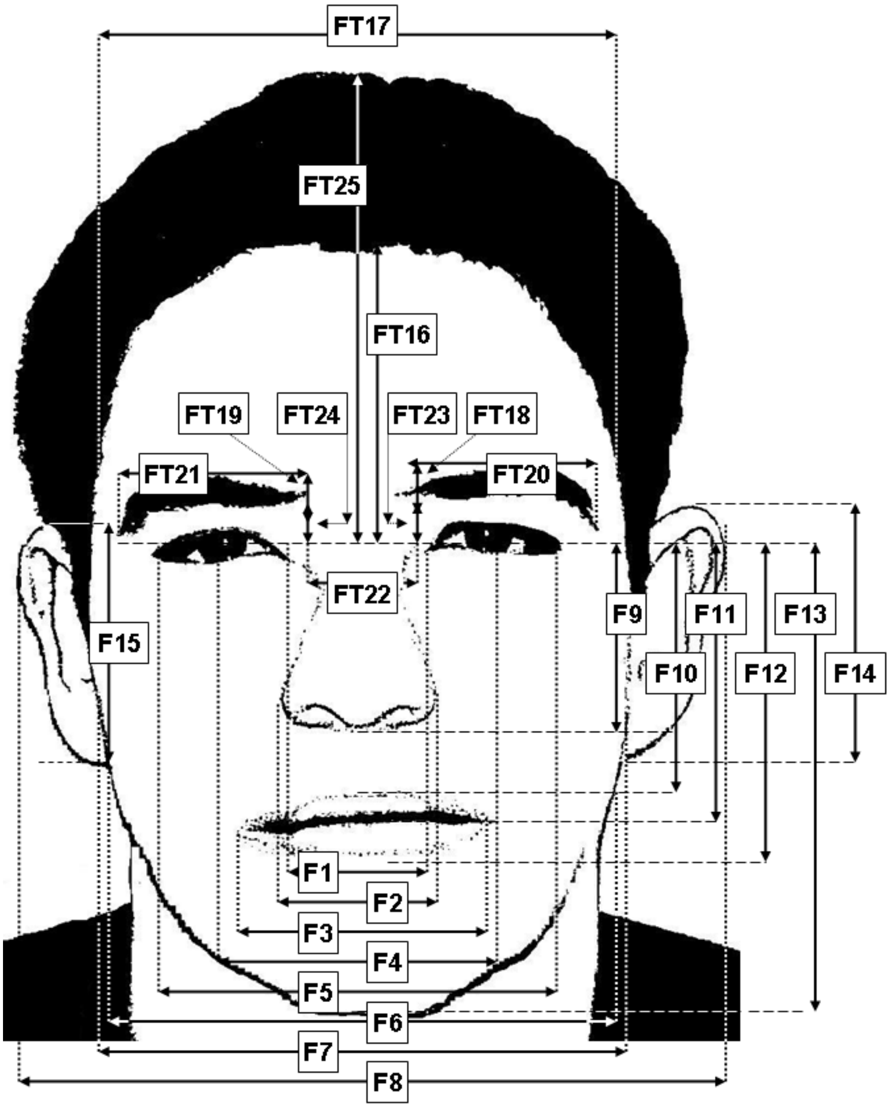

Permanent horizontal distances *(see Figure 1 for key to landmark numbers*)			
F1	Distance between inner eyes (1 – 2)	F2	Nose width (9 – 10)
F3	Mouth width (11 – 12)	F4	Inter-pupil distance (3 – 4)
F5	Distance between outer eyes (5 – 6)	F6	Face width at upper lip height (14 – 15)
F7	Face width at nostril height (17 – 18)	F8	Distance between outer ears (7 – 8)
Permanent vertical distances			
F9	Eye line to nose base (1/2 – 19)	F10	Eye line to upper lip (1/2 – 13)
F11	Eye line to mouth centre (1/2 – 20)	F12	Eye line to lower lip (1/2 – 21)
F13	Eye line to chin (1/2 – 22)	F14	Right ear height (23 - 24)
F15	Left ear height (25 - 26)		
Transient distances			
FT16	Eye line to hairline (1/2 – 27)	FT17	Face width at top eyebrow (29 – 30)
FT18	Right eyebrow height (28 - 31)	FT19	Left eyebrow height (32 - 33)
FT20	Right eyebrow width (34 - 35)	FT21	Left eyebrow width (36 - 37)
FT22	Distance between eyebrows (34 - 36)	FT23	Eye line to right eyebrow (1/2 – 31)
FT24	Eye line to left eyebrow (1/2 – 33)	FT25	Eye line to top of head (1/2 – 38)

Figure 4: Permanent and transient (marked with a T) distance measures produced by DigitalFace in profile view

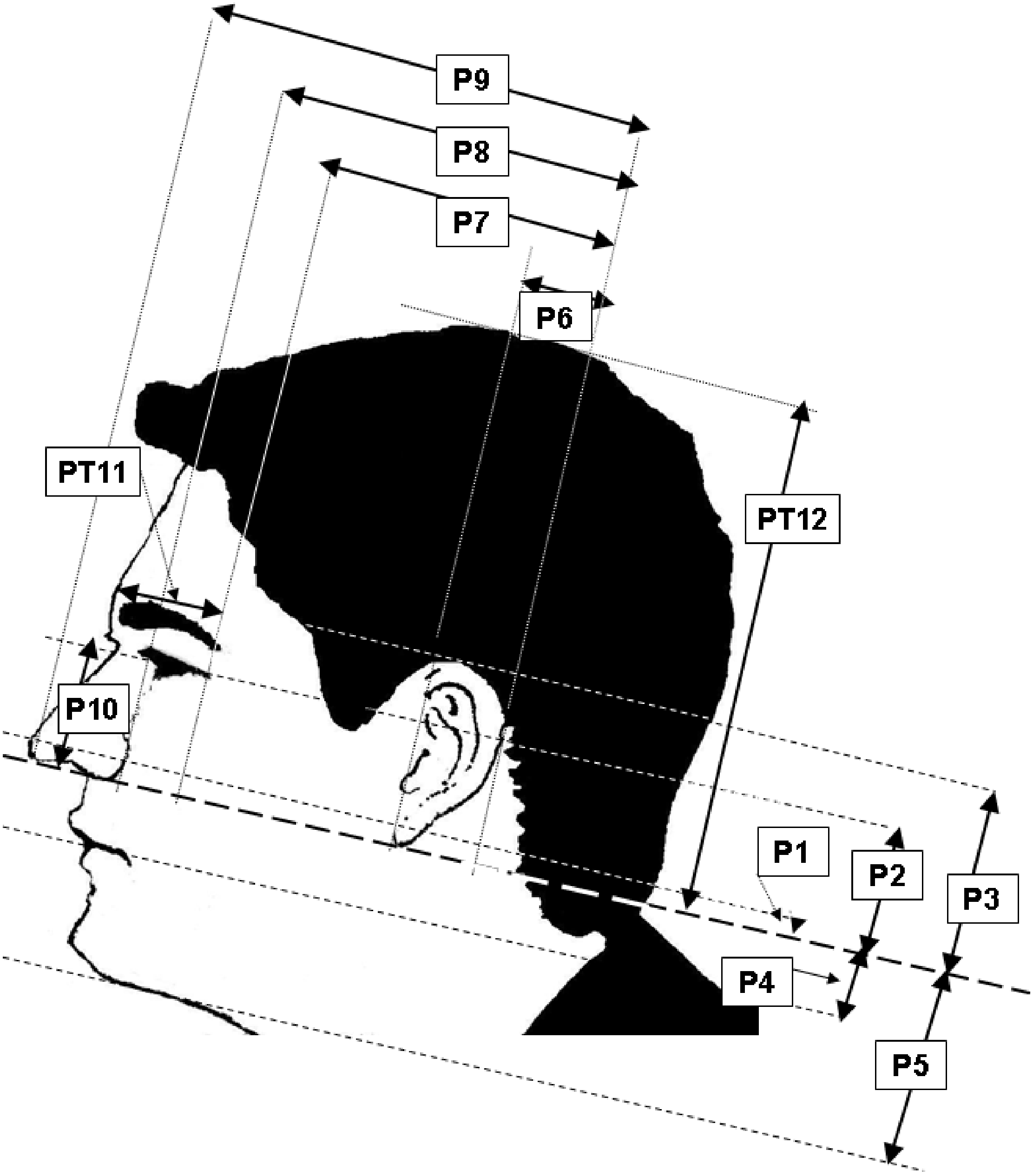

Permanent vertical distances (see Figure 2 for key to landmark numbers)			
P1	Nose/ear base line to nose tip (1/2– 3)	P2	Nose/ear base line to eye (1/2–4)
P3	Nose/ear base line to top ear (1/2–5)	P4	Nose/ear base line to mouth (1/2 – 6)
P5	Nose/ear base line to chin (1/2 – 7)		
Permanent horizontal distances			
P6	Ear width (8 – 9)	P7	Rear of ear to outer eye (8 – 4)
P8	Rear of ear to rear of nose (8 – 10)	P9	Rear of ear to nose tip (8 – 3)
P10	Nose height (3 – 11)		
Transient distances			
PT11	Eyebrow width (12 – 13)	PT12	Nose/ear base line to head (1/2 – 14)

Figure 5: Full-face angular measurements computed by DigitalFace

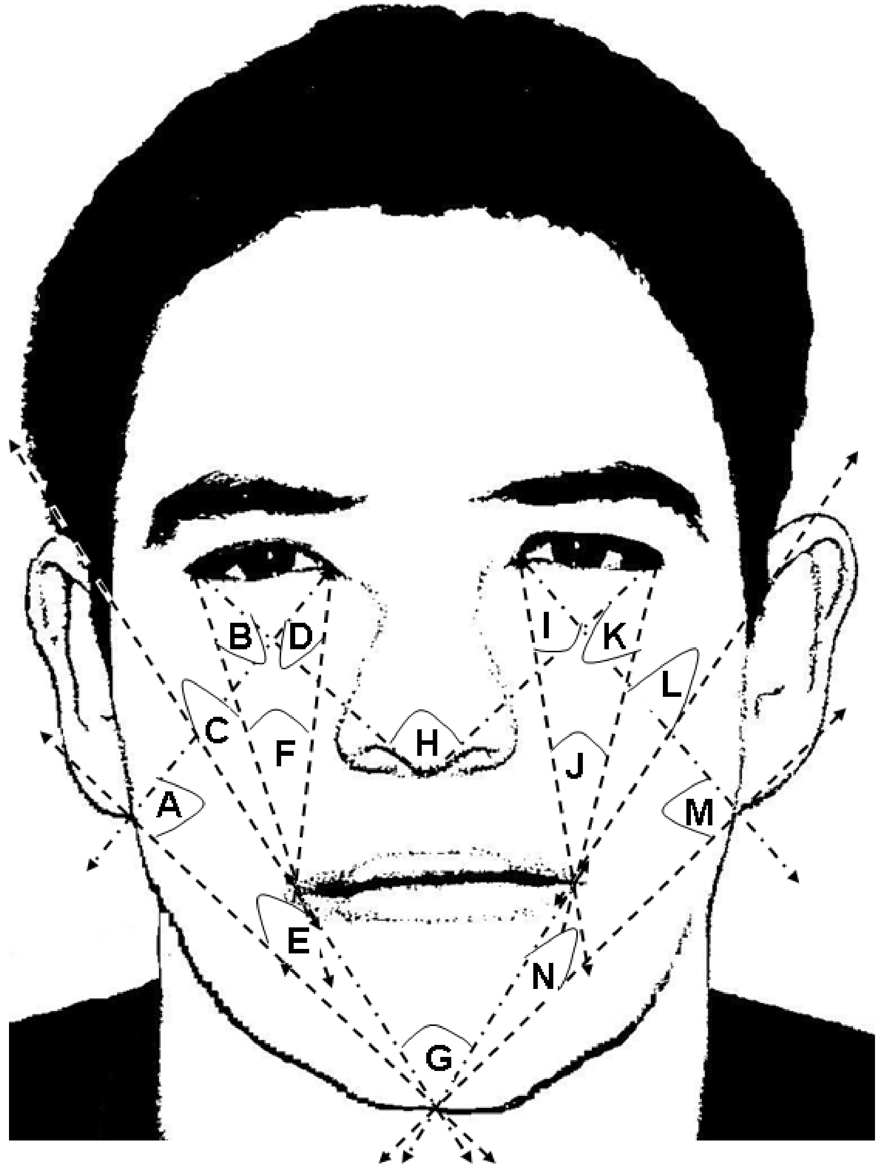

Angle	Connecting lines (see Figure 1 for key to landmark numbers)							
A	2	(left inner eye)	-	26	(left ear base)	-	22	(chin)
B	12	(left mouth)	-	6	(left outer eye)	-	19	(nose base)
C	6	(left outer eye)	-	12	(left mouth)	-	25	(left ear top)
D	12	(left mouth)	-	2	(left inner eye)	-	26	(left ear base)
E	25	(left ear top)	-	22	(chin)	-	26	(left ear base)
F	2	(left inner eye)	-	12	(left mouth)	-	6	(left outer eye)
G	11	(right mouth)	-	22	(chin)	-	12	(left mouth)
H	5	(right outer eye)	-	19	(nose base)	-	6	(left outer eye)
I	11	(right mouth)	-	1	(right inner eye)	-	24	(right ear base)
J	1	(right inner eye)	-	11	(right mouth)	-	5	(right outer eye)
K	11	(right mouth)	-	5	(right outer eye)	-	19	(nose base)
L	5	(right outer eye)	-	11	(right mouth)	-	23	(right ear top)
M	1	(right inner eye)	-	24	(right ear base)	-	22	(chin)
N	11	(right mouth)	-	22	(chin)	-	24	(right ear base)

Figure 6: Profile angular measurements computed by DigitalFace

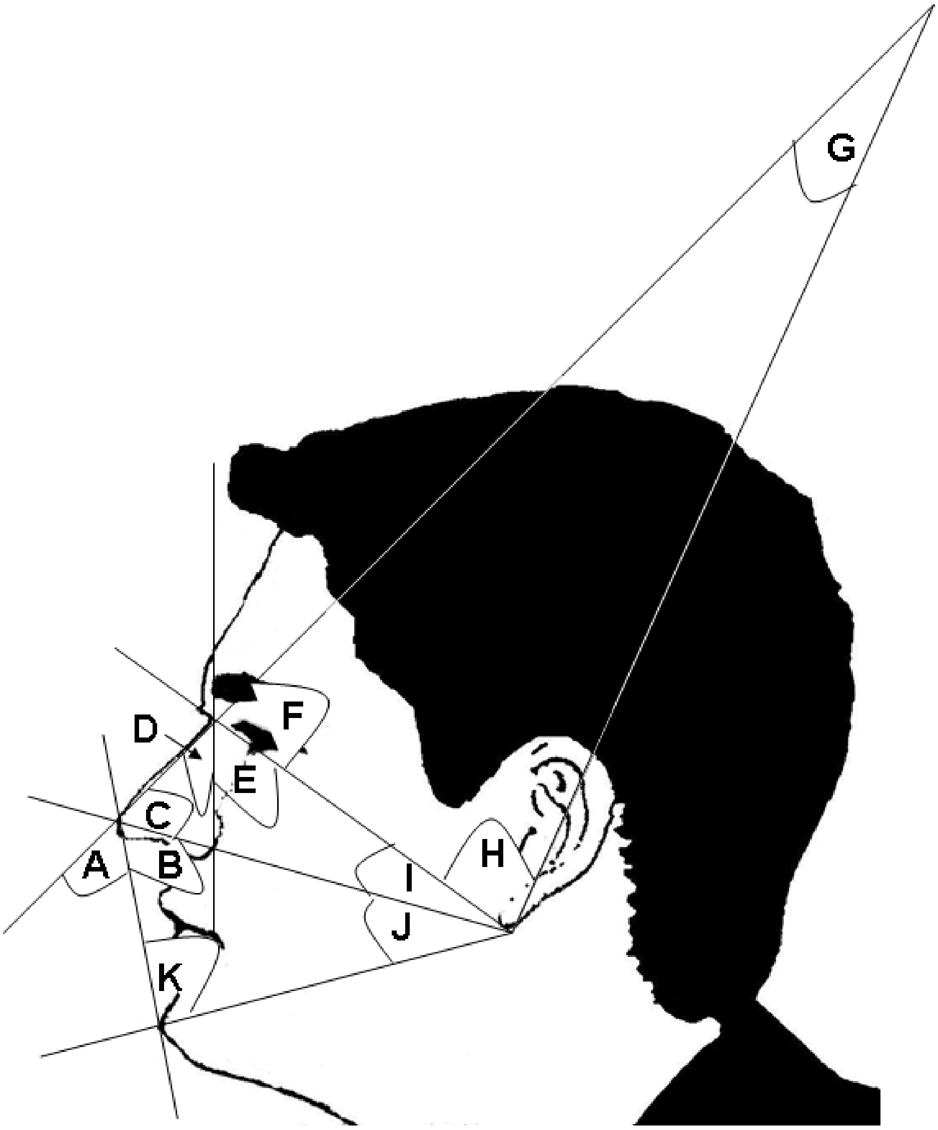

Angle	Connecting lines (see Figure 2 for key to landmark numbers)							
A	7	(chin)	-	3	(nose tip)	-	11	(top of nose)
B	2	(ear base)	-	3	(nose tip)	-	7	(chin)
C	2	(ear base)	-	3	(nose tip)	-	11	(top of nose)
D	3	(nose tip)	-	11	(top of nose)	-	10	(rear nose)
E	2	(ear base)	-	11	(top of nose)	-	6	(mouth corner)
F	2	(ear base)	-	11	(top of nose)	-	3	(nose tip)
G	3	(nose tip)	-	11	(top of nose)	-	2	(ear base)
H	4	(outer eye)	-	2	(ear base)	-	5	(top of ear)
I	3	(nose tip)	-	2	(ear base)	-	4	(outer eye)
J	3	(nose tip)	-	2	(ear base)	-	7	(chin)
K	2	(ear base)	-	7	(chin)	-	3	(nose tip)

Annex 1

Orthogonal distance between a point and a line

To calculate the distance between a point and the nearest point to it on a straight line

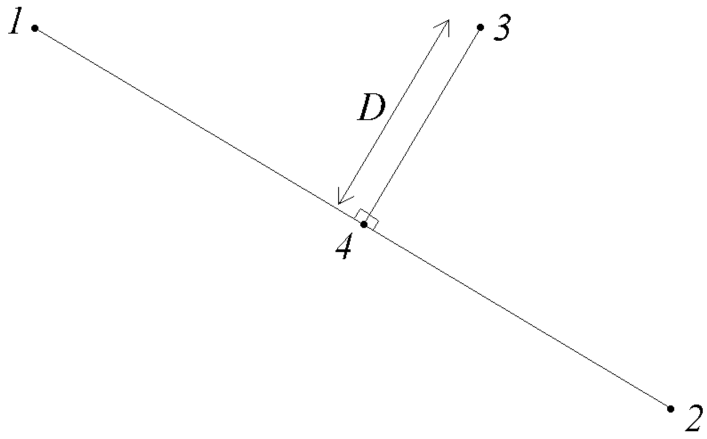

If coordinates of the points in the above diagram are:

$1 = x_1y_1$
$2 = x_2y_2$
$3 = x_ty_t$
$4 = x_uy_u$

First generate equations for the lines of the form $y = mx + c$:

Line *12*:

$m_a = (y_2 - y_1)/(x_2 - x_1)$
$C_a = y_1 - m_a\, x_1$

Line *34*:

$m_b = -1/m_a$
$C_b = y_t - m_bx_t$

At *4*:

$x_a = x_b = x_u$ and $y_a = y_b = y_u$

So:

$m_ax_u + C_a = m_bx_u + C_b$
$m_ax_u - m_bx_u = C_b - C_a$
$x_u(m_a - m_b) = C_b - C_a$
$x_u = (C_b - C_a)/(m_a - m_b)$
$y_u = m_ax_u + C_a$

$D = \sqrt{((x_u - x_t)^2 + (y_u - y_t)^2)}$